SIAM J. APPL. MATH.
Vol. 70, No. 4, pp. 1157–1177

FILTRATION COMBUSTION IN WET POROUS MEDIUM*

J. BRUINING†, A. A. MAILYBAEV‡, AND D. MARCHESIN§

Abstract. We consider the filtration combustion for configuration where air is injected behind the wave into a porous medium containing a solid fuel. The simplest flow contains planar combustion and thermal waves, each propagating with its own speed. In this work, we study such a flow, in the case where the porous medium contains initially also some amount of liquid; therefore, vaporization and condensation occur too, giving rise to a wave structure richer than in dry combustion. We find two possible sequences of waves, and we characterize the internal structure of all waves. In an example for typical parameters of in-situ combustion, we compare the analytical results with direct numerical simulations.

Key words. filtration combustion, traveling wave, porous medium, evaporation, condensation, conservation law

AMS subject classifications. 80A25, 76S05, 35L65

DOI. 10.1137/080741318

1. Introduction.

Combustion of solid fuel in porous medium when the oxidizer (air) is injected has numerous applications in technology and nature (self-propagating high-temperature synthesis, smolder waves, etc.). In this paper we study the case when some liquid is initially present in the porous medium, which occurs in coal gasification and in-situ combustion in oil recovery. The liquid gets vaporized by the combustion front, it moves with the injected gas, and it condenses when it reaches the cold zone ahead of the combustion wave. The heat necessary for liquid vaporization is generated by the combustion, and the liquid concentration ahead of the combustion front increases due to the vapor condensation. Therefore, combustion, vaporization, and condensation are coupled.

Analysis of the reaction layer (RL) represents the main mathematical difficulty in the study of filtration combustion. We follow the approach developed in [10, 11, 13] for various combustion conditions; see also the application of this method for filtration combustion of coke in [1]. In this approach, it is assumed that the RL is thin and that the reaction stops due to low temperature on one side of this layer, which is called cold boundary condition. Since the reaction does not stop completely at low temperatures, the resulting solution is of transient type. However, it represents a slowly varying "traveling wave" that is observed in many practical applications. In this case, classical conservation law theory, the method of characteristics, fractional flow theory, or rigorous traveling wave analysis cannot be applied directly. In our study, we consider only waves traveling with constant speed. Stability of the obtained solution

*Received by the editors November 19, 2008; accepted for publication (in revised form) June 22, 2009; published electronically September 18, 2009. This work partially supported by CNPq under grants 301532/2003-6, 491148/2005-4, 472067/2006-0, 304168/2006-8, 300668/2007-4, 474121/2008-9, 68.018/2008-5, 453973/2008-6, CAPES under grant 0854-11/2007, FAPERJ under grants E-26/152.525/2006, E-26/102.723/2008, and the President of Russian Federation grant MK-4244.2008.1.

http://www.siam.org/journals/siap/70-4/74131.html

†TU Delft, Civil Engineering and Geosciences, Stevinweg 1, 2628 CE Delft, The Netherlands (j.bruining@tudelft.nl).

‡Institute of Mechanics, Moscow State University, Michurinsky pr. 1, 119192 Moscow, Russia (mailybaev@imec.msu.ru).

§Instituto Nacional de Matemática Pura e Aplicada, Estrada Dona Castorina 110, 22460-320 Rio de Janeiro, RJ, Brazil (marchesi@impa.br).

is checked numerically for specific problem parameters. Of course, for different system parameters, this solution may become unstable, extinguishing or giving rise to many interesting phenomena such as periodic or chaotic regimes; see, e.g., [9, 3].

A related problem when the water is injected together with air into a dry reservoir was studied by Dietz and Weijdema [6]. They showed the existence of a steam zone between the combustion and condensation waves. With the increase of the water/air injection ratio, the evaporation wave and combustion wave start to coincide, leading to the process called partially quenched combustion. Partially quenched combustion was demonstrated in the laboratory. In our case, rather than injected, the water is initially present in the reservoir, yielding a different wave structure.

In our problem, we assume that the region swept by the combustion front contains initially a small amount of liquid that is immobile. This can be water, or even a combustible liquid. Thus, besides regular combustion, the main effect taken into account is the liquid evaporation and condensation. Two types of wave sequence solutions arise depending on initial reservoir and injection parameters. These solutions are characterized by complete consumption of either fuel or oxygen. The condition for liquid vapor to be completely expelled from the reaction area is derived. It is crucial for our analysis to apply when the liquid is combustible.

We describe the model in section 2. In section 3, we investigate the case of complete fuel consumption in the combustion. The analytic solution is obtained, determining the temperature changes in thermal, combustion-vaporization, and condensation waves. Here the combustion-vaporization wave is the traveling wave with an intermediate layer of heat conduction. Combustion and vaporization occur in thin layers of this wave. In section 4, we present a numerical example for typical parameters of in-situ combustion and compare the analytical results with numerical simulation. In section 5, we study the case of complete oxygen consumption in the combustion. In this case the analytic solution includes separate vaporization, combustion, and condensation waves. Here we also perform numerical analysis for typical parameters of in-situ combustion. The results are discussed in the conclusion.

2. Model. Consider a porous rock cylinder thermally insulated on the side and filled with inert gas, vaporizable liquid, and combustible solid fuel. An oxidizer (air) is injected. The liquid can be water or light oil, and the combustible solid can be coke. We assume that the amount of liquid is small, so its mobility is negligible. We assume that only a small part of the available space is occupied by solid fuel and liquid, so that we can neglect changes of rock porosity in the reaction, evaporation, and condensation processes. We assume that the solid, liquid, and gas are in local thermal equilibrium, so they have the same temperature.

A one-dimensional model with time t and space coordinate x is considered. The heat transport equation is

$$\frac{\partial C(T-T_{res})}{\partial t} + \frac{\partial c_g \rho u (T-T_{res})}{\partial x} = \lambda \frac{\partial^2 T}{\partial x^2} + Q_r W_r - Q_e W_e, \tag{2.1}$$

where T [K] is the temperature and T_{res} is the initial reservoir temperature, ρ [mole/m^3] is the *molar* density of gas, u [m/s] is the Darcy velocity of gas, C [J/m^{3}K] is the heat capacity per unit volume, c_g [J/mole K] is the heat capacity of gas per mole, λ [W/mK] is the thermal conductivity of the porous medium, Q_r, Q_e [J/mole] are, respectively, the heats (enthalpies) of combustion and evaporation of the solid and the liquid at reservoir temperature T_{res}, and W_r, W_e [mole/m^{3}s] are the reaction and evaporation rates per unit volume of porous medium.

Note that the form of the left-hand side of (2.1) corresponds to constant enthalpies Q_r, Q_e taken at reservoir temperature T_{res}. If these enthalpies are evaluated at the actual temperature T, the left-hand side becomes $C\partial T/\partial t + c_g\rho u\partial T/\partial x$, as one can show using the mass balance equations given below. We take C equal to the heat capacity of the rock matrix per unit volume of porous medium C_m (disregarding the heat capacity of solid fuel, liquid, and gas in the pores).

We consider a single component liquid (e.g., water), and denote by X its vapor molar fraction in the gas phase (mole of vapor/mole of gas). The gas has several components: vapor, oxygen, and passive (inert and combusted) gas. We denote the molar fractions of oxygen and passive gas in the gas-phase by Y and Z, respectively. Then, we write the mass balance equations for the components X, Y, Z as (see, e.g., [5])

$$\varphi\frac{\partial X\rho}{\partial t} + \frac{\partial X\rho u}{\partial x} = D_X\varphi\frac{\partial}{\partial x}\rho\frac{\partial X}{\partial x} + W_e, \tag{2.2}$$

$$\varphi\frac{\partial Y\rho}{\partial t} + \frac{\partial Y\rho u}{\partial x} = D_Y\varphi\frac{\partial}{\partial x}\rho\frac{\partial Y}{\partial x} - \mu_o W_r, \tag{2.3}$$

$$\varphi\frac{\partial Z\rho}{\partial t} + \frac{\partial Z\rho u}{\partial x} = D_Z\varphi\frac{\partial}{\partial x}\rho\frac{\partial Z}{\partial x} + \mu_g W_r, \tag{2.4}$$

where φ is the porosity and D_X, D_Y, D_Z [m^2/s] are the diffusion coefficients for vapor, oxygen, and passive gas in the gaseous phase. As a first approximation, we assume that $D_X = D_Y = D_Z = D$ (however, see the Stefan–Maxwell relations in [4] for the full composition dependence). Using that the sum of mole fractions $X+Y+Z$ is equal to one, we obtain the mass balance equation for the total gas

$$\varphi\frac{\partial \rho}{\partial t} + \frac{\partial \rho u}{\partial x} = (\mu_g - \mu_o)W_r + W_e. \tag{2.5}$$

As the solid fuel and the liquid do not move, their concentrations satisfy the equations for reaction and evaporation, respectively:

$$\frac{\partial n_f}{\partial t} = -\mu_f W_r, \tag{2.6}$$

$$\frac{\partial n_l}{\partial t} = -W_e, \tag{2.7}$$

where n_f, n_l [mole/m^3 of porous medium] are the molar concentrations of solid fuel and liquid. In the combustion reaction, μ_f moles of solid fuel react with μ_o moles of oxygen and generate μ_g moles of gaseous products. Below, we assume that the stoichiometric coefficients are $\mu_f = \mu_o = \mu_g = 1$, as in the reaction $C + O_2 \to CO_2$.

The ideal gas law for the gaseous phase has the form

$$P_{tot} = \rho RT, \tag{2.8}$$

with the ideal gas constant $R = 8.314$ [J/mole K] and the prevailing pressure P_{tot} [Pa]. Assuming that the variation of pressure in the flow is small, we take $P_{tot} = \text{const}$. The vapor pressure in thermodynamic equilibrium with the liquid is described by the Clausius–Clapeyron relation

$$P_X = P_{atm}\exp\left(-\frac{Q_e}{R}\left(\frac{1}{T} - \frac{1}{T_b}\right)\right) \tag{2.9}$$

valid in the region containing liquid, where T_b is the boiling temperature of the liquid at atmospheric pressure P_{atm} and $P_X = X_{eq}P_{tot}$ is the partial pressure of vapor in equilibrium with its liquid at the temperature T. With the ideal gas law, we can express the equilibrium mole fraction of vapor X_{eq} in the gas as

$$X_{eq}(T) = \frac{P_X}{P_{tot}} = \frac{P_{atm}}{P_{tot}} \exp\left(-\frac{Q_e}{R}\left(\frac{1}{T} - \frac{1}{T_b}\right)\right). \tag{2.10}$$

The evaporation (condensation) rate can be taken as

$$W_e = kn_l(X_{eq}(T) - X), \tag{2.11}$$

where the equilibrium vapor fraction $X_{eq}(T)$ is computed by (2.10). The coefficient k can be different for $X < X_{eq}$ (evaporation) and $X > X_{eq}$ (condensation). Below, we will assume that k is large, so that liquid and vapor are always in equilibrium: $X \approx X_{eq}(T)$.

We use the Arrhenius law and the first order law of mass action in the reaction rate

$$W_r = K_r Y n_f \exp\left(-\frac{E_r}{RT}\right) \tag{2.12}$$

with the constant activation energy E_r [J/mole] and the preexponential parameter K_r [1/s], which is also assumed to be constant.

The variables to be found are the temperature T, the molar concentrations of solid fuel n_f and liquid n_l, the molar fractions of oxygen and vapor Y, X, and the Darcy velocity u. The quantities C_m, c_g, λ, D, Q_r, Q_e are assumed to be constant (neglecting the dependence on temperature and gas composition).

2.1. Dimensionless equations. The equations are nondimensionalized by introducing dimensionless dependent and independent variables (denoted by tildes) as a ratio of the dimensional quantities and reference quantities (denoted by stars):

$$\tilde{t} = \frac{t}{t^*}, \quad \tilde{x} = \frac{x}{x^*}, \quad \theta = \frac{T - T_{res}}{T^*}, \quad \tilde{\rho} = \frac{\rho}{\rho^*}, \quad \tilde{n}_{f,l} = \frac{n_{f,l}}{n^*_{f,l}}, \quad \tilde{u} = \frac{u}{u^*}. \tag{2.13}$$

Let us take $v^* = c_g\rho^* u_{inj}/C_m$, which turns out to be the speed of the thermal wave (a wave where temperature changes with no reaction). Then we introduce the reference length and time as $x^* = \lambda/(C_m v^*)$ and $t^* = x^*/v^*$, which are appropriate for the thermal wave. The temperature change for combustion under adiabatic conditions can be used as the characteristic temperature $T^* = Q_r n_f^*/C_m$. Thus, our choice for reference quantities is

$$\begin{gathered} t^* = \frac{x^*}{v^*}, \quad x^* = \frac{\lambda}{C_m v^*}, \quad v^* = \frac{c_g\rho^* u_{inj}}{C_m}, \quad T^* = \frac{Q_r n_f^*}{C_m}, \quad \rho^* = \frac{P_{tot}}{RT_{res}}, \\ n_f^* = n_f^{res}, \quad n_l^* = n_l^{res}, \quad u^* = u_{inj}, \end{gathered} \tag{2.14}$$

where T_{res} and $n_{f,l}^{res}$ are the initial reservoir temperature and fuel, liquid concentrations, respectively, and u_{inj} is the injected gas velocity. Using (2.13), (2.14), and omitting the tildes, (2.1)–(2.10) are written in dimensionless form as

$$\frac{\partial\theta}{\partial t} + \frac{\partial\rho u\theta}{\partial x} = \frac{\partial^2\theta}{\partial x^2} + w_r - \beta w_e, \tag{2.15}$$

$$\frac{\partial \rho}{\partial t} + \sigma \frac{\partial \rho u}{\partial x} = \gamma_l w_e, \tag{2.16}$$

$$\frac{\partial Y\rho}{\partial t} + \sigma \frac{\partial Y\rho u}{\partial x} = \frac{1}{\mathrm{Le}} \frac{\partial}{\partial x} \rho \frac{\partial Y}{\partial x} - \gamma_f w_r, \tag{2.17}$$

$$\frac{\partial X\rho}{\partial t} + \sigma \frac{\partial X\rho u}{\partial x} = \frac{1}{\mathrm{Le}} \frac{\partial}{\partial x} \rho \frac{\partial X}{\partial x} + \gamma_l w_e, \tag{2.18}$$

$$\frac{\partial n_f}{\partial t} = -w_r, \tag{2.19}$$

$$\frac{\partial n_l}{\partial t} = -w_e, \tag{2.20}$$

$$\rho(\theta + \theta_0) = \theta_0, \tag{2.21}$$

$$X_{eq} = \alpha \exp\left(-\frac{h}{\theta + \theta_0}\right), \tag{2.22}$$

with dimensionless constants

(2.23)
$$\mathrm{Le} = \frac{\lambda}{C_m D}, \quad N_{Da} = K_r t^*, \quad \gamma_{f,l} = \frac{n^*_{f,l}}{\varphi \rho^*}, \quad \sigma = \frac{u^*}{\varphi v^*}, \quad \beta = \frac{Q_e n^*_l}{Q_r n^*_f}, \quad h = \frac{Q_e}{RT^*},$$
$$\mathcal{E} = \frac{E}{RT^*}, \quad \kappa = t^* k, \quad \theta_0 = \frac{T_{res}}{T^*}, \quad \alpha = \frac{P_{atm}}{P_{tot}} \exp\left(\frac{Q_e}{RT_b}\right).$$

Here Le is the Lewis number, N_{Da} is the Damkohler number, γ_f and γ_l characterize the initial fuel and liquid concentrations relative to the gas density, σ is the interstitial gas velocity relative to the thermal wave velocity, and β gives the ratio of evaporation and combustion heats for total amounts of liquid and fuel. We omitted the dimensionless form of (2.4) as $Z = 1 - X - Y$.

The dimensionless reaction and evaporation rates are given by $w_r = t^* W_r / n^*_f$ and $w_e = t^* W_e / n^*_l$. The evaporation rate (2.11) takes the form

$$w_e = \kappa n_l (X_{eq}(\theta) - X). \tag{2.24}$$

For the reaction rate (2.12), we get the dimensionless expression

$$w_r = N_{Da} Y n_f \exp\left(-\frac{\mathcal{E}}{\theta + \theta_0}\right). \tag{2.25}$$

3. Wave sequence for complete fuel consumption. In this section, we study the solution having a structure shown in Figure 1. The solution consists of three waves along which the temperature varies, besides a much faster wave with constant temperature. These waves are separated by zones with constant states.

The slowest (first from left to right) is a thermal wave, where the temperature raises to a high value θ_h. Ahead of this wave, there is a constant hot zone. The second is a combustion-vaporization wave, which consists of a reaction layer (RL) and a vaporization layer (VL) joined by an intermediate heating layer (HL). Behind the RL, the reaction stops due to lack of fuel (*complete fuel consumption*). Ahead of the RL, the reaction does not start because the reaction rate is negligible at low temperature. We will see that, under rather general conditions (explicitly specified), all the liquid vaporizes in the VL, and none of its vapor remains in the reaction area.

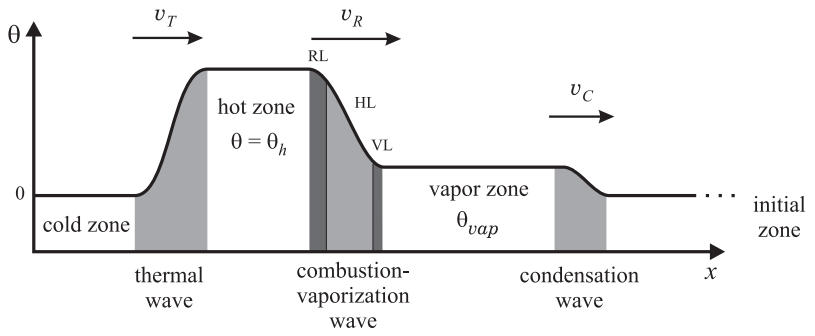

FIG. 1. *Wave sequence for complete fuel consumption.*

For such flows, it makes no difference whether the liquid is combustible or not. For example, the liquid initially present in the reservoir can be water or light oil.

The zone ahead of the combustion-vaporization wave contains liquid in equilibrium with its vapor in the transported gas. This zone ends at a condensation wave. There is also a composition wave that travels with the speed of the gas, which is much larger than the speeds of the other waves, so that this wave does not fit in Figure 1. Along this wave, the concentrations of unburned oxygen and of combusted gases drop to zero, while the temperature and total gas flux do not change. To the right of this wave, there is gas at initial reservoir composition, as well as initial reservoir liquid.

The boundary conditions at the left injection side determine the temperature, gas flux, and oxygen concentration:

$$x = 0,\ t \geq 0: \quad \theta = 0, \quad \rho = u = 1, \quad Y_{inj}, \quad X = 0, \tag{3.1}$$

where we assumed that the injected gas temperature is equal to the initial reservoir temperature. The last condition in (3.1) means that there is no vapor in the injected gas. The initial data in the reservoir determine the temperature, fuel, and liquid concentrations

$$x \geq 0,\ t = 0: \quad \theta = 0, \quad n_f = n_l = 1, \quad X_{res} = \alpha \exp(-h/\theta_0), \tag{3.2}$$

where X_{res} is determined by (2.22) by replacing θ by zero.

Complete fuel consumption implies that the condition $n_f = 0$ holds behind the combustion-vaporization wave. Complete consumption of oxygen in the injected gas when it seeps through the RL is not required, and the concentration of the unburned oxygen ahead of the combustion-vaporization wave is denoted by Y_{unb}. Neither liquid nor vapor are left behind this wave: $n_l = X = 0$.

3.1. Thermal wave. The first wave is described by (2.15) and (2.16) in the absence of reaction and evaporation

$$\frac{\partial \theta}{\partial t} + \frac{\partial \rho u \theta}{\partial x} = \frac{\partial^2 \theta}{\partial x^2}, \tag{3.3}$$

$$\frac{\partial \rho}{\partial t} + \sigma \frac{\partial \rho u}{\partial x} = 0. \tag{3.4}$$

Since neither vapor, liquid, nor fuel are left behind the combustion-vaporization wave, we have $X = n_l = n_f = 0$. The oxygen concentration $Y = Y_{inj}$ does not change in

the thermal wave (the corresponding equation (2.17) is trivially satisfied). The rock and gas heat capacities are very different, so $\sigma = u^*/(\varphi v^*) = C_m/(\varphi c_g \rho^*) \gg 1$, and we can neglect the first term in (3.4). This shows that the flux ρu is independent of x. Using the boundary conditions (3.1), we find $\rho u \equiv 1$. Then (3.3) takes the form

$$\frac{\partial \theta}{\partial t} + \frac{\partial \theta}{\partial x} = \frac{\partial^2 \theta}{\partial x^2}. \tag{3.5}$$

In the solution of (3.5), the temperature θ tends to zero as $x \to -\infty$ and to θ_h as $x \to \infty$:

$$\theta(t,x) = \frac{\theta_h}{2} + \frac{\theta_h}{2} \operatorname{erf}\left(\frac{x - x_T - v_T t}{2\sqrt{t}}\right), \qquad v_T = 1, \tag{3.6}$$

where x_T is the wave position at $t = 0$ and $\operatorname{erf}(x) = (2/\sqrt{\pi}) \int_0^x e^{-\xi^2} d\xi$; recall that $\operatorname{erf}(\infty) = -\operatorname{erf}(-\infty) = 1$. The wave travels with speed $v_T = 1$. Thus, the dimensional speed v^* given in (2.14) is indeed the thermal wave speed. The width of the wave grows proportionally to $\sqrt{t}$ due to heat conduction.

The state in the hot zone (ahead of the thermal wave) is

$$\text{Hot zone}: \quad \theta = \theta_h, \quad \rho u = 1, \quad Y = Y_{inj}, \quad X = n_f = n_l = 0, \tag{3.7}$$

where θ_h is unknown. By using (2.21), we also find $\rho = 1/u = \theta_0/(\theta_h + \theta_0)$.

3.2. Combustion-vaporization wave. According to the wave structure in Figure 1, we conjecture that the reaction and vaporization take place in a single traveling wave. The wave travels with speed v_R and consists of an RL and a VL, joined by an intermediate HL. In the RL, the solid fuel reacts with oxygen: $w_r > 0$, $w_e = 0$. In the VL, the liquid vaporizes: $w_r = 0$, $w_e > 0$. Finally, in the HL we have $w_r = w_e = 0$. The combustion-vaporization wave is faster than the thermal wave, which implies

$$v_R > 1. \tag{3.8}$$

Let us introduce the traveling coordinate $\xi = x - x_R - v_R t$, where x_R is the wave position at $t = 0$. We choose the origin so that the RL, HL, and VL correspond to $\xi < 0$, $0 < \xi < L$, and $\xi > L$, respectively. All the state variables in the wave depend only on ξ; prime will denote the derivative with respect to ξ. At the ends of the wave ($\xi \to \pm\infty$), the derivatives with respect to ξ vanish.

3.2.1. RL. In the RL, there is neither liquid nor vapor ($n_l = X = w_e = 0$), and (2.15)–(2.20) in the traveling coordinate yield

$$(\rho u \theta - v_R \theta)' = \theta'' + w_r, \tag{3.9}$$

$$(\sigma \rho u - v_R \rho)' = 0, \tag{3.10}$$

$$(\sigma Y \rho u - v_R Y \rho)' = \frac{(\rho Y')'}{Le} - \gamma_f w_r, \tag{3.11}$$

$$v_R n_f' = w_r; \tag{3.12}$$

while (2.18) is satisfied trivially for $X = w_e = 0$. Assuming that

$$v_R \ll \sigma u \tag{3.13}$$

(typically $v_R \sim v_T = 1$, $u \sim 1$, and $\sigma \gg 1$), we neglect the term with v_R in (3.10) and (3.11). Then (3.10) yields constant flux, which is $\rho u \equiv 1$ because of (3.7). We substitute w_r from (3.12) into (3.9), (3.11) and integrate taking into account the boundary conditions (3.7) and $\theta' = Y' = 0$ at $\xi \to -\infty$, yielding

$$\theta' + (v_R - 1)(\theta - \theta_h) + v_R n_f = 0, \tag{3.14}$$

$$\frac{\rho Y'}{Le} + \sigma(Y_{inj} - Y) - v_R \gamma_f n_f = 0. \tag{3.15}$$

We obtained the system of ordinary differential equations (3.12), (3.14), (3.15) governing the RL. Its analytical study requires further simplifications.

Since the activation energy is usually very large ($\mathcal{E} \gg 1$), the reaction rate (2.25) is determined mainly by the exponential factor, and the reaction occurs for θ close to its upper limit θ_h, where the exponent is large. Thus, the exponential expression can be written approximately as

$$-\frac{\mathcal{E}}{\theta + \theta_0} \approx -\frac{\mathcal{E}}{\theta + \theta_h} + \frac{\mathcal{E}\,\delta\theta}{(\theta + \theta_0)^2}, \qquad \delta\theta = \theta - \theta_h. \tag{3.16}$$

The characteristic change of temperature in the RL, corresponding to change by 1 in the exponential expression (3.16), is

$$\delta\theta_R = \frac{(\theta_h + \theta_0)^2}{\mathcal{E}}. \tag{3.17}$$

This quantity is assumed to be small; its dimensional expression according to (2.14) and (2.23) is

$$\delta\theta_R = \frac{R T_h^2}{T^* E} \ll 1, \tag{3.18}$$

where T_h is the dimensional temperature of combustion. Note that $\delta\theta_R$ represents the inverse Zeldovich number, which is the ratio of the total temperature change and the temperature change in the RL.

Using (3.18), we can neglect the second term in (3.14) compared to the third term: $(v_R - 1)(\theta - \theta_h) \lesssim v_R \delta\theta_R \ll v_R \sim v_R n_f$; see (3.8). So (3.14) reads

$$\theta' = -v_R n_f. \tag{3.19}$$

The effective length of the RL can be found by taking $\theta' \approx -\delta\theta_R / l_R$ in (3.19) with $n_f \sim 1/2$ and using (3.17) as

$$l_R = \frac{2\delta\theta_R}{v_R} = \frac{2(\theta_h + \theta_0)^2}{v_R \mathcal{E}}. \tag{3.20}$$

Let us consider (3.15). The magnitude of the first term is estimated as $\rho Y'/Le \sim \delta Y/(l_R Le)$, where δY is the change of Y in the RL (recall that the dimensionless dependent variables ρ, θ, n_f, n_l are of order 1). We can distinguish two extreme cases that allow analytical study: (a) when the diffusion term in (3.15) is small, and (b) when it is dominant:

$$\text{(a):}\ \ Le\, l_R \sigma \gg 1, \qquad \text{(b):}\ \ Le\, l_R \sigma \ll 1. \tag{3.21}$$

Using (2.14), (2.23), we express $Le\, l_R\sigma$ in terms of dimensional parameters as $l_R u_{inj}/\varphi D$ (with dimensional length l_R); this is the mass diffusion Péclet number for the RL.

We assume that the reaction does not start ahead of the RL because the temperature is low (despite the presence of both fuel and oxygen). Strictly speaking, the RL does not have a sharp border, but rather there is a continuous passage from the RL to the HL. The assumptions (3.18), (3.21) allow finding an approximate analytical solution for the RL that later must be patched with the solution in the HL.

First, consider case (a); see Figure 2. The diffusion term in (3.15) is small and can be neglected. Expression (3.15) takes the form

$$Y = Y_{inj} - v_R\gamma_f n_f/\sigma. \tag{3.22}$$

Dividing θ' from (3.19) by n_f' from (3.12), using (2.25) and (3.22), we obtain

$$\exp\left(-\frac{\mathcal{E}}{\theta+\theta_0}\right)d\theta = -\frac{v_R^2}{N_{Da}}\frac{dn_f}{Y_{inj} - v_R\gamma_f n_f/\sigma}. \tag{3.23}$$

This equation can be integrated from the left-hand side of the RL ($\theta = \theta_h$, $n_f = 0$) to its right-hand side ($\theta = \theta_2 < \theta_h$, $n_f = 1$):

$$\int_{\theta_2}^{\theta_h}\exp\left(-\frac{\mathcal{E}}{\theta+\theta_0}\right)d\theta = \frac{v_R^2}{N_{Da}}\int_0^1 \frac{dn_f}{Y_{inj} - v_R\gamma_f n_f/\sigma}. \tag{3.24}$$

The main contribution to the integral in the left-hand side is given by θ close to the upper limit θ_h when the exponent is large. We compute this integral approximately using (3.16) and integrating with respect to $\delta\theta$ from $-\infty$ to 0:

$$\int_{\theta_2}^{\theta_h}\exp\left(-\frac{\mathcal{E}}{\theta+\theta_0}\right)d\theta \approx \frac{(\theta_h+\theta_0)^2}{\mathcal{E}}\exp\left(-\frac{\mathcal{E}}{\theta_h+\theta_0}\right). \tag{3.25}$$

Integrating the right-hand side in (3.24), we obtain

$$\frac{(\theta_h+\theta_0)^2}{\mathcal{E}}\exp\left(-\frac{\mathcal{E}}{\theta_h+\theta_0}\right) = \frac{v_R\sigma}{N_{Da}\gamma_f}\log\frac{Y_{inj}}{Y_{unb}}. \tag{3.26}$$

Here the fraction of unburned oxygen in the gas ahead of the RL is found from (3.22) by taking $n_f = 1$. It is

$$Y_{unb} = Y_{inj} - v_R\gamma_f/\sigma. \tag{3.27}$$

Now consider case (b) in (3.21); see Figure 2. The magnitude of the first term in (3.15) is $\rho Y'/Le \sim \delta Y/(l_R Le)$. Comparing this expression with the second term and using condition (b) in (3.21), we find $\delta Y \ll Y_{inj} - Y$. Thus, we can take $Y = \text{const}$ approximately in the RL; this constant must be equal to the amount of unburned oxygen Y_{unb} ahead of the RL. Y_{unb} is given by the same equation (3.27), which just reflects the reaction equation ($v_R\gamma_f/\sigma$ is the amount of oxygen necessary for complete fuel combustion). As there is no reaction behind the RL, the concentration Y increases exponentially to the value Y_{inj} behind the RL, as determined by the equation $(\rho Y)'/Le - \sigma(Y - Y_{inj}) = 0$. Thus, in case (b), we substitute the denominator $Y_{inj} - v_R\gamma_f n_f/\sigma$ in (3.23) by Y_{unb}. The analysis now leads to the following equation instead of (3.26):

$$\frac{(\theta_h+\theta_0)^2}{\mathcal{E}}\exp\left(-\frac{\mathcal{E}}{\theta_h+\theta_0}\right) = \frac{v_R^2}{N_{Da}Y_{unb}}. \tag{3.28}$$

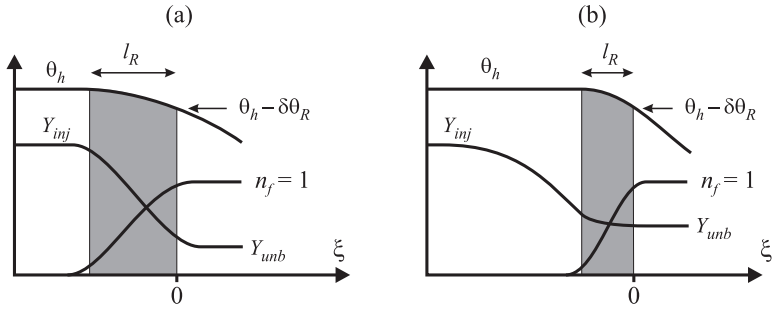

FIG. 2. *Structure of the reaction layer (RL) for small diffusion* (a) *and dominant diffusion* (b).

We set the traveling coordinate origin $\xi = 0$ at the right-hand side of the RL. As the temperature variation is small across the RL, we can take $\theta \approx \theta_h$ at $\xi = 0$. So, we have

$$\begin{aligned} \xi = 0: \quad & \theta = \theta_h, \quad \theta' = -v_R, \quad \rho u = 1, \\ & X = 0, \quad Y_{unb} = Y_{inj} - v_R \gamma_f/\sigma, \quad n_f = 1, \quad n_l = 0. \end{aligned} \tag{3.29}$$

Here we used expressions (3.19) and (3.27). The condition $n_l = 0$ (no liquid) follows from the assumption that $\theta > \theta_b$. For $\xi > 0$, we will neglect the oxidation reaction, as its rate is very small at low temperatures.

3.2.2. Intermediate layer. The HL lies in the interval $0 < \xi < L$. In the HL, there is neither reaction nor vaporization: $w_r = w_e = 0$, and the gas flux is constant $\rho u \equiv 1$. The main phenomenon is heat transfer. The traveling wave is determined by the heat equation (2.15) as

$$(1 - v_R)\theta' = \theta'', \tag{3.30}$$

which is the same as (3.9) with $w_r = 0$. The general solution of this equation has the form

$$\theta = \alpha_0 + \alpha_1 \exp(-A\xi), \qquad A = v_R - 1 > 0. \tag{3.31}$$

The values of θ and θ' at $\xi = 0$ are given in (3.29), yielding

$$\alpha_0 = \theta_h - \alpha_1, \qquad \alpha_1 = v_R/A. \tag{3.32}$$

Let us denote the values of θ, θ' at $\xi = L$ by θ_L, θ'_L. Using (3.31), (3.32),

$$\theta_L = \theta_h - \frac{v_R}{A}(1 - e^{-AL}), \qquad \theta'_L = -v_R e^{-AL}. \tag{3.33}$$

The traveling wave form of (2.18) in the HL is

$$\sigma X' = \frac{(\rho X')'}{Le}, \tag{3.34}$$

where we used (3.13) and the conditions $w_e = 0$ and $\rho u = 1$. Under the assumption (verified in section 3.2.4) that the vapor concentration becomes very small at $\xi = 0$ so that $X \approx 0$ and $X' \approx 0$, we integrate (3.34) and obtain

$$X' = Le\, \sigma X/\rho. \tag{3.35}$$

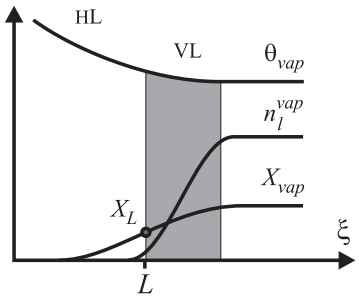

FIG. 3. *Structure of the VL.*

A second integration of (3.35) with the condition $X = X_L$ at $\xi = L$ yields

$$X = X_L \exp\left(-\int_\xi^L \frac{\sigma\, Le}{\rho} d\xi\right), \tag{3.36}$$

where $\rho = \theta_0/(\theta + \theta_0)$ according to (2.21); see Figure 3.

3.2.3. VL. The VL starts at $\xi = L$; see Figure 3. In the VL, we have $w_e > 0$ and $w_r = 0$. Equations (2.15), (2.16), (2.18), (2.20) in the traveling wave coordinate $\xi = x - x_R - v_R t$ take the form

$$(\rho u\theta - v_R\theta)' = \theta'' - \beta w_e, \tag{3.37}$$

$$\sigma(\rho u)' = \gamma_l w_e, \tag{3.38}$$

$$\sigma(X\rho u)' = \frac{(\rho X')'}{Le} + \gamma_l w_e, \tag{3.39}$$

$$v_R n_l' = w_e. \tag{3.40}$$

In the derivation of (3.38) and (3.39), we neglected the terms with v_R according to (3.13); (2.19) is trivially satisfied.

First, let us estimate the VL structure parameters, assuming that the two terms on the right-hand side of each of (3.37) and (3.39) are of same order. Comparing these terms and using (2.24), we find $\delta\theta_V/l_V^2 \sim \beta\kappa\,\delta X_V$ and $1/(l_V^2 Le) \sim \gamma_l\kappa$, where δX_V denotes the change of X in the VL and l_V is the effective length of the VL. From (3.40) we obtain $v_R/l_V \sim \kappa\,\delta X_V$. Expressing l_V from the second relation and then δX_V and $\delta\theta_V$ from the third and first relations, respectively, we derive the estimates

$$\delta\theta_V \sim \frac{\beta v_R}{\sqrt{Le\,\gamma_l\kappa}}, \quad l_V \sim \frac{1}{\sqrt{Le\,\gamma_l\kappa}}, \quad \delta X_V \sim v_R\sqrt{\frac{Le\,\gamma_l}{\kappa}}. \tag{3.41}$$

We assume that the vaporization process is fast, i.e., κ is large. According to (3.41), this means that both $\delta\theta_V$ and l_V are small. Under this assumption, we take $\theta \approx \theta_{vap}$. We also neglect the term in the left-hand side of (3.37) compared to the large term $\theta'' \sim \delta\theta_V/l_V^2$ proportional to $\kappa^{1/2}$. (Quantitative conditions for these simplifications, obtained by comparing the corresponding terms in the equations, are $\delta\theta_V \ll 1$ and $c_g(T_{vap} - T_{res})/Q_e \ll 1$.) Substituting w_e from (3.40) into (3.37)–(3.39) and integrating over the VL yields

$$[\theta'] - \beta v_R n_l^{vap} = 0, \tag{3.42}$$

$$\sigma[\rho u] - \gamma_l v_R n_l^{vap} = 0, \tag{3.43}$$

$$\frac{\rho_{vap}}{Le}[X'] - \sigma[X\rho u] + \gamma_l v_R n_l^{vap} = 0, \tag{3.44}$$

where $\rho_{vap} = \theta_0/(\theta_{vap}+\theta_0)$ and the square brackets denote the change of the quantity across the layer; we took into account that $[n_l] = n_l^{vap}$ is the liquid concentration ahead of the wave; see Figure 3.

Ahead of the VL (in the vapor zone) we have $\theta' = 0$, $\rho u = (\rho u)_{vap}$, $X = X_{vap}$, and $X' = 0$. Behind the VL, $\theta' = \theta'_L$, $\rho u = 1$, $X = X_L$, and $X' = X'_L$. Expression (3.35) gives $X'_L = Le\,\sigma X_L/\rho_{vap}$. Along the VL we have $\theta \approx \theta_{vap}$. Using all these conditions in (3.42)–(3.44), elementary calculations yield behind the VL (at $\xi = L$)

$$\theta_L = \theta_{vap}, \qquad \theta'_L = -\beta v_R n_l^{vap}, \tag{3.45}$$

and ahead of the VL (in the vapor zone)

$$(\rho u)_{vap} = 1 + \gamma_l v_R n_l^{vap}/\sigma, \qquad X_{vap} = (1 + \sigma/(\gamma_l v_R n_l^{vap}))^{-1}. \tag{3.46}$$

Using (3.45) with $A = v_R - 1$ in (3.33) yields the expression for θ_{vap}:

$$\theta_{vap} = \theta_h - \frac{v_R(1 - \beta n_l^{vap})}{v_R - 1}, \tag{3.47}$$

and the HL length

$$L = -\frac{\log(\beta n_l^{vap})}{v_R - 1}. \tag{3.48}$$

The equilibrium condition (2.22) in the vapor zone reads

$$X_{vap} = \alpha \exp\left(-\frac{h}{\theta_{vap} + \theta_0}\right). \tag{3.49}$$

Since we neglect the oxidation in the HL and VL, the oxygen flux is constant in the traveling frame within these layers: $(\sigma u - v_R)Y\rho \approx \sigma Y \rho u = \text{const}$; see (3.13). Thus, the mole fraction of oxygen in the vapor zone ahead of the combustion-vaporization wave can be computed from the condition $Y_{vap}(\rho u)_{vap} = Y_{unb}$, where $(\rho u)_{vap}$ is given in (3.46).

3.2.4. Defining equations. Here we summarize the equations for the combustion-vaporization wave. There are six defining equations: (3.27), (3.46), (3.47), (3.49), and, depending on the case, (3.26) or (3.28). They relate the values of seven unknown variables: θ_h, θ_{vap}, X_{vap}, Y_{unb}, n_l^{vap}, $(\rho u)_{vap}$, and the wave speed v_R. According to the classification of the conservation law theory, the combustion-vaporization wave is a so-called transitional, or undercompressive wave, as it possesses one extra free variable compared to classical Lax waves; see [7, 8].

The following conditions are necessary for the existence of the combustion-vaporization wave. Using (3.8) and (3.27) in the inequality $Y_{unb} \geq 0$, we obtain the condition

$$Y_{inj}\sigma/\gamma_f \geq 1. \tag{3.50}$$

This inequality coincides with the condition for complete fuel consumption in the absence of liquid given in [13]. The equality $Y_{inj}\sigma/\gamma_f = 1$ corresponds to the resonant combustion regime when both the fuel and oxygen are totally consumed in the

reaction. As $Y_{inj} \to \gamma_f/\sigma$ and $Y_{unb} \to 0$, (3.27) yields $v_R \to 1$. In this case, the denominator in (3.47) tends to zero. This implies that the combustion temperature θ_h becomes very large. The study of the resonant combustion regime done in [2] shows that the combustion temperature increases in time proportionally to $\sqrt{t}$. Our analysis is not applicable to the case of resonance: for high temperatures, heat losses must be taken into account.

Another condition is obtained by using (3.48) in the inequality $L > 0$, viz.,

$$\beta n_l^{vap} < 1. \tag{3.51}$$

Since β gives the ratio between the evaporation and combustion heats (see (2.23)), this inequality requires that the heat of combustion must be sufficient to evaporate all the liquid.

Finally, we assumed that the vapor does not enter the RL. This assumption is crucial when the vapor is combustible; otherwise, the solution would be different. The vapor concentration in the HL is given by (3.36). The assumption that the vapor does not enter the RL is equivalent to the condition $X \ll 1$ at $\xi = 0$. Since $\rho > 1$ and $X_L < X_{vap}$ in the vaporization process, the condition is satisfied if

$$X_{vap} \exp(-\sigma Le\, L) \ll 1. \tag{3.52}$$

Using (2.14), (2.23), we see that the exponent $\sigma Le\, L$ in dimensional form is $Lu_{inj}/\varphi D$ (with dimensional L); this is the mass diffusion Péclet number for the HL. Thus, condition (3.52) is satisfied if this number is large. Note that if the vapor is combustible, it can also react with oxygen in the vapor zone, where the temperature is higher than the initial reservoir temperature. Our solution is valid only under the assumption that this reaction is negligible.

3.3. Condensation wave. The vapor zone between the combustion-vaporization wave and condensation wave contains liquid with concentration $n_l = n_l^{vap}$ in equilibrium with vapor at concentration X_{vap}, which is related to θ_{vap} by (2.22).

The condensation wave travels with speed v_C. Equations (2.15)–(2.20) for the traveling wave yield (3.37)–(3.40) with v_R substituted by v_C. They are the same as for the vaporization layer in section 3.2.3, but the derivative is taken with respect to the new traveling coordinate $\xi = x - x_C - v_C t$. Substituting n_l' from (3.40) into (3.37)–(3.39) and integrating over the condensation wave gives

$$[\rho u \theta] - v_C[\theta] - \beta v_C(n_l^{vap} - 1) = 0, \tag{3.53}$$

$$\sigma[\rho u] + \gamma_l v_C(n_l^{vap} - 1) = 0, \tag{3.54}$$

$$\sigma[X\rho u] + \gamma_l v_C(n_l^{vap} - 1) = 0, \tag{3.55}$$

where we used that $\theta' = X' = 0$ on both sides and $[n_l] = 1 - n_l^{vap}$, since the reservoir initial liquid concentration is $n_l = 1$. Using expression (3.46) for the gas flux behind the wave $(\rho u)_{vap}$ in (3.54), the gas flux ahead of the wave is

$$\rho u = 1 + \gamma_l v_R n_l^{vap}/\sigma - \gamma_l v_C(n_l^{vap} - 1)/\sigma. \tag{3.56}$$

Ahead of the wave, $X = X_{res}$ and ρu is given by (3.56); behind the wave, $X = X_{vap}$ and ρu are given by (3.46). Thus, (3.55) takes the form

$$\sigma X_{res} + \gamma_l(v_R n_l^{vap} - v_C(n_l^{vap} - 1))X_{res} - \gamma_l v_R n_l^{vap} + \gamma_l v_C(n_l^{vap} - 1) = 0. \tag{3.57}$$

Then we find

$$n_l^{vap} = \frac{\gamma_l v_C - \sigma X_{res}/(1-X_{res})}{\gamma_l (v_C - v_R)}. \tag{3.58}$$

Since ahead of the wave $\theta = 0$, behind the wave $\theta = \theta_{vap}$ and ρu is given by (3.46), (3.53) takes the form

$$\theta_{vap}\,(v_C - 1 - \gamma_l v_R n_l^{vap}/\sigma) = \beta v_C (n_l^{vap} - 1). \tag{3.59}$$

The oxygen flux does not change in the condensation wave. Similarly to the vaporization layer, this yields the condition $Y\rho u = \text{const} = Y_{unb}$. Thus, the oxygen fraction ahead of the combustion wave is $Y = Y_{unb}/\rho u$, where ρu is given in (3.56).

In the above analysis we assumed that $n_l^{vap} > 1$, i.e., the liquid concentration in the vapor zone is higher than in the initial reservoir. If $n_l^{vap} < 1$, the structure of the solution changes. This is the case when the initial liquid concentration is so small that vaporization at low temperatures (unrelated to combustion front) becomes dominant. We do not study this case in the paper.

3.4. Defining system of equations for the wave sequence. The wave sequence is determined by a system of nonlinear algebraic equations (3.26)–(3.28) and (3.47), (3.59):

$$\frac{(\theta_h+\theta_0)^2}{\mathcal{E}} \exp\left(-\frac{\mathcal{E}}{\theta_h+\theta_0}\right) = \begin{cases} \dfrac{v_R\sigma}{N_{Da}\gamma_f} \log \dfrac{Y_{inj}}{Y_{inj} - v_R\gamma_f/\sigma}, & \text{case (a);} \\ \dfrac{v_R^2}{N_{Da}(Y_{inj} - v_R\gamma_f/\sigma)}, & \text{case (b);} \end{cases} \tag{3.60}$$

$$\theta_{vap} = \theta_h - v_R(1 - \beta n_l^{vap})/(v_R - 1); \tag{3.61}$$

$$\theta_{vap}\,(v_C - 1 - \gamma_l v_R n_l^{vap}/\sigma) = \beta v_C (n_l^{vap} - 1). \tag{3.62}$$

In (3.61) and (3.62) one should use θ_{vap} obtained from (3.49), (3.46) as

$$\theta_{vap} = h/\log(\alpha/X_{vap}) - \theta_0, \qquad X_{vap} = (1 + \sigma/(\gamma_l v_R n_l^{vap}))^{-1}, \tag{3.63}$$

and substitute n_l^{vap} from (3.58). Therefore, (3.60)–(3.62) contains three unknowns: the combustion temperature θ_h and the wave speeds v_R, v_C. This nonlinear system must be solved numerically. In numerical calculations, it is useful to know that $v_R < Y_{inj}\sigma/\gamma_f$, which follows from (3.27) with $Y_{unb} > 0$. Having found θ_h, v_R, and v_C, expressions (3.27), (3.46)–(3.49), (3.56), and (3.58) determine the other solution parameters.

Remark. When there is no vaporizable liquid in the porous medium, the vaporization layer and the condensation wave disappear. The combustion wave is characterized by (3.60), (3.61) with θ_{vap} and n_l^{vap} replaced by zero. Substituting θ_h from the second resulting equation into the first one, we obtain a single transcendental equation for the wave speed, which lies in the interval $1 < v_R < Y_{inj}\sigma/\gamma_f$. This equation corresponds to the studies [2, 13] in the case (a) and to the studies [1, 10] in the case (b). Our results complement these studies by giving appropriate conditions (3.21), (3.20), distinguishing the cases when diffusion is negligible in the reaction layer (a) and when diffusion is dominant (b).

Necessary conditions for the existence of the solution with wave sequence described above include the inequalities (3.50) and (3.51) for the combustion-vaporization wave. An extra condition follows from the assumption $n_l^{vap} \geq 1$ necessary for the existence of a separate condensation wave.

4. Numerical results for typical reservoir data. Numerical computations were carried out for typical parameters of in-situ combustion with petroleum coke fuel and water; see [1, 12]. The dimensional parameters are given in Table 1. The corresponding reference quantities and dimensionless parameters are

(4.1)

$$t^* = 2.62\,\text{days}, \quad x^* = 0.314\,\text{m}, \quad T^* = 197.5\,\text{K}, \quad v^* = 0.120\,\text{m/day},$$
$$Le = 2.175 \times 10^{-2}, \quad N_{Da} = 2.26 \times 10^{13}, \quad \gamma_f = 67.7, \quad \gamma_l = 180.5, \quad \sigma = 5.56 \times 10^3,$$
$$\beta = 0.228, \quad h = 24.7, \quad \mathcal{E} = 97.4, \quad \kappa = 2.26 \times 10^3, \quad \theta_0 = 1.48, \quad \alpha = 4.83 \times 10^5.$$

Solving (3.60)–(3.62) numerically with the data (4.1), we obtain the wave sequence parameters given in the second row of Table 2. We used the formula of case (a), since the quantity in condition (3.21) is $Le\, l_R \sigma = 22.5 \gg 1$, with $l_R = 0.196$ computed using (3.20). In the condition (3.52), we have $X_{vap} \exp(-\sigma Le\, L) \sim 10^{-135} \ll 1$, with $L = 2.53$ found using (3.48). This condition guarantees that no vapor enters the reaction layer. We can expect that the same conclusion is generally true for liquid fuels, so the latter do not participate in the combustion.

For comparison, the numerical simulation was carried out using a split-implicit finite difference scheme for the PDE system (2.15)–(2.20). The steady solution obtained using numerical simulation is presented in Figure 4, where the temperature θ with

TABLE 1
Typical values of the dimensional parameters for in-situ combustion.

Parameters	Values
Q_r	4.74×10^5 J/mole of carbon
Q_e	4.06×10^4 J/mole,
E	1.6×10^5 J/mole
K_r	10^8 1/s
R	8.314 J/mole K
C_m	2×10^6 J/m^{3}K
λ	0.87 W/mK
D	$2 \times 10^{-5}(P_{atm}/P_{tot})$ m^2/s
c_g	29.2 J/mole K
φ	0.3
P_{tot}	10^5 Pa (1 atm)
Y_{inj}	0.21 mole of O_2/mole of air
n_f^{res}	833.3 mole/m^3 (10 kg of carbon per m^3)
n_l^{res}	2222 mole/m^3 (40 kg of water per m^3)
T_b	373.15 K (water),
T_{res}	293.15 K
u_{inj}	200 m/day
k	0.01 1/s

TABLE 2
Parameters of the wave sequence solution obtained by analytical formulae and numerical simulation.

	θ_h	v_R	Y_{unb}	θ_{vap}	v_C	X_{vap}	n_l^{vap}
Analytic	2.212	1.507	0.192	0.064	4.400	0.056	1.213
Numeric	2.220	1.536	0.192	0.060	4.404	0.054	1.200

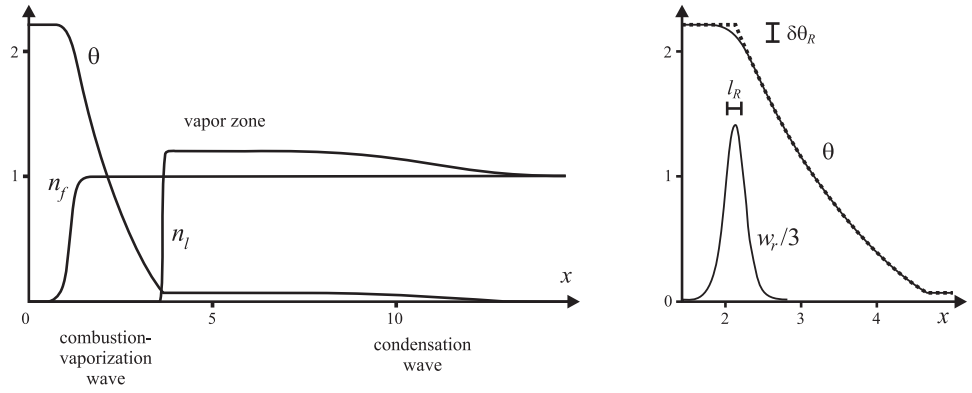

FIG. 4. *Nondimensional results of numerical simulation for combustion-vaporization and condensation waves.*

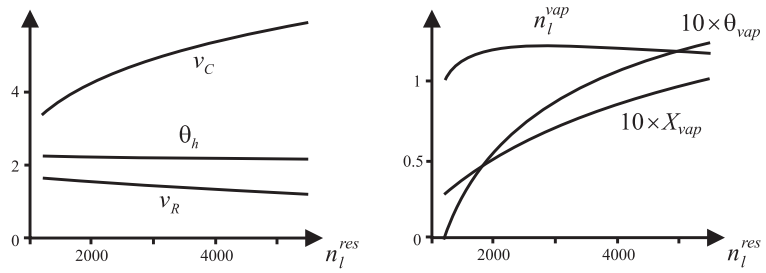

FIG. 5. *Nondimensional solution parameters depending on the initial water concentration* $n_l^{res}[mole/m^3]$.

the fuel concentration n_f and water concentration n_l are shown. The combustion-vaporization and condensation wave are well distinguished on the figure (the thermal wave on the left is not shown). The solution parameters can be read from the simulation profiles; they are given in the third row of Table 2. One can see that they are in very good agreement with the analytic values shown in the second row. On the plot at the right of Figure 4, we compare the analytical temperature profile given by (3.31) (bold dotted line) with the numerical simulation (solid line) for the combustion-vaporization wave; we also show here the reaction rate w_r and the characteristic dimensions of the reaction layer (3.17), (3.20).

Finally, Figure 5 shows the dependence of the solution parameters on the initial liquid concentration changed in the interval $1205 < n_l^{res} < 5500$ [mole/m^3]. Here the upper bound $n_l^{res} = 5500\,\text{mole/m}^3$ corresponds approximately to $100\,\text{kg/m}^3$ of water. For $n_l^{res} < 1205\,\text{mole/m}^3$, we have $n_l^{vap} < 1$, so that the condensation does not occur. One can see that the waves speeds v_R and v_C are sensitive to the liquid concentration, while the combustion temperature θ_h is not.

5. Complete oxygen consumption wave sequence. In this section, we study the solution with structure shown in Figure 6. The solution consists of three waves along which the temperature varies, besides a much faster wave with constant temperature. These waves are separated by zones with constant states. The slowest is a combustion wave. Ahead of the reaction layer, lack of oxygen due to its complete consumption prevents the reaction. Behind the reaction layer, the reaction stops because of low temperature, where the reaction rate is negligible. Ahead of this wave,

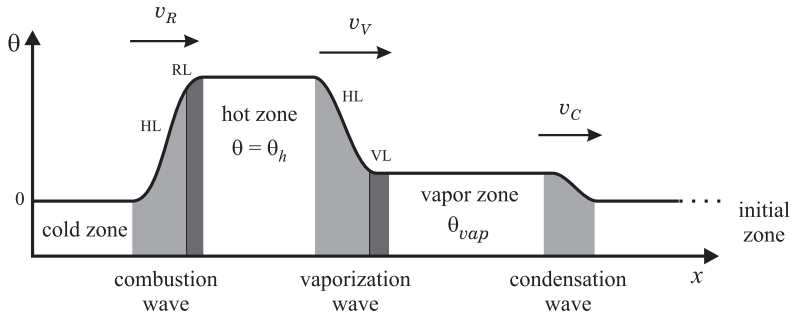

FIG. 6. *Wave sequence for complete oxygen consumption.*

we have a hot zone with temperature θ_h. The second wave is a vaporization wave: here the temperature drops to θ_{vap}, and the liquid vaporizes in the front part of the wave. The zone ahead of this wave contains liquid in equilibrium with its vapor in the transported gas. This zone ends with a condensation wave. There is also a composition wave where the concentration of gaseous products of combustion drops to zero. This wave travels with the speed of the gas, which is much larger than the speeds of the other waves, so that this wave does not fit in Figure 6.

The injection conditions at the left side and the initial reservoir conditions are given in (3.1), (3.2). The assumption of complete oxygen consumption implies that the condition $Y = 0$ holds ahead of the combustion wave. Complete fuel consumption is not required, and the concentration of unburned fuel is denoted by n_f^{unb}. The assumption of complete liquid vaporization yields the condition $n_l = X = 0$ everywhere behind the vaporization wave.

In this section, we give the derivations in short form, as they are essentially similar to those in section 3.

5.1. Combustion wave. The combustion wave is a traveling wave with speed v_R. As before, we introduce the traveling coordinate $\xi = x - x_R - v_R t$. Behind the wave, we have the injection conditions (3.1) and an unknown amount of unburned solid fuel $n_f = n_f^{unb}$. Ahead of the wave (as $\xi \to \infty$), we have $\theta = \theta_h$, $n_f = 1$, and the condition of complete oxygen consumption $Y = 0$. All the derivatives with respect to ξ vanish as $\xi \to \pm\infty$.

The equations describing the reaction layer in the combustion wave are (3.9)–(3.12). Assuming $v_R \ll \sigma u$, the constant gas flux condition $\rho u \equiv 1$ is derived first. Then, equations analogous to (3.14), (3.15) using the new boundary conditions ($\theta' = Y' = 0$, $\theta = \theta_h$, $n_f = 1$, $Y = 0$ ahead of the wave) become

$$\theta' - (1 - v_R)(\theta - \theta_h) - v_R(1 - n_f) = 0, \tag{5.1}$$

$$\frac{\rho Y'}{Le} - \sigma Y + v_R \gamma_f (1 - n_f) = 0. \tag{5.2}$$

As we will see soon, $v_R < 1$.

We distinguish two layers. In the RL, the reaction occurs at temperature close to θ_h. Behind the RL, there is an HL, where there is no reaction and the temperature drops to its value $\theta = 0$ in the injected gas; see Figure 6. To allow explicit analysis, let us assume that

$$\frac{\delta\theta_R}{v_R(1 - n_f^{unb})} \ll 1, \qquad Le\, l_R \sigma \gg 1. \tag{5.3}$$

As in section 3.2.1, we use conditions (5.3) to neglect the second term in (5.1) $(1-v_R)(\theta-\theta_h) \lesssim \delta\theta_R$ compared to the third term $v_R(1-n_f)$, and the first term in (5.2) $\rho Y'/Le \sim Y_{inj}/(Le\, l_R)$ compared to the second term $\sigma Y \sim \sigma Y_{inj}$. These simplifications yield

$$Y = v_R\gamma_f(1-n_f)/\sigma, \qquad \theta' = v_R(1-n_f). \tag{5.4}$$

Let us choose $\xi = 0$ between HL and RL. At $\xi = 0$, we have $n_f = n_f^{unb}$, $Y = Y_{inj}$, and $\theta \approx \theta_h$. Using (5.4) we obtain

$$\xi = 0: \quad \theta = \theta_h, \quad n_f^{unb} = 1 - \sigma Y_{inj}/(v_R\gamma_f), \quad \theta' = \sigma Y_{inj}/\gamma_f. \tag{5.5}$$

Dividing θ' from (5.4) by n_f' from (3.12), using (2.25) and expression (5.4) for Y, we obtain

$$\exp\left(-\frac{\mathcal{E}}{\theta+\theta_0}\right) d\theta = \frac{v_R\sigma}{N_{Da}\gamma_f}\frac{dn_f}{n_f}. \tag{5.6}$$

This equation is integrated as in section 3.2.1, which yields

$$\frac{(\theta_h+\theta_0)^2}{\mathcal{E}} \exp\left(-\frac{\mathcal{E}}{\theta_h+\theta_0}\right) = -\frac{v_R\sigma}{N_{Da}\gamma_f} \log\left(1-\frac{\sigma Y_{inj}}{v_R\gamma_f}\right), \tag{5.7}$$

where we used expression (5.5) for n_f^{unb}.

For the effective change of temperature $\delta\theta_R$ in the RL, we get the same relation (3.17). Taking $\theta' \sim \delta\theta_R/l_R$ in the second relation in (5.4), we estimate the RL length as $l_R \sim \delta\theta_R/(v_R(1-n_f^{unb}))$.

In the HL, the reaction is neglected: $w_r = 0$. Behind the wave, the temperature decreases to $\theta \to 0$. The change of the temperature is given by the expression

$$\theta = \alpha_0 + \alpha_1 \exp(-A\xi), \qquad A = v_R - 1, \tag{5.8}$$

which is found as for the HL in section 3.2.2. Since the temperature increases together with ξ, the constant A must be negative. This gives the condition $v_R < 1$, the opposite of condition (3.8) for complete fuel consumption. From the condition $\theta = 0$ behind the wave and the third equation in (5.5), we find

$$\alpha_0 = 0, \qquad \alpha_1 = \frac{\sigma Y_{inj}}{(1-v_R)\gamma_f}. \tag{5.9}$$

Then the first relation in (5.5) with θ given by (5.8), (5.9) yields

$$\theta_h = \frac{\sigma Y_{inj}}{(1-v_R)\gamma_f}. \tag{5.10}$$

Equations (5.7) and (5.10) determine the temperature θ_h, and the combustion wave speed v_R for given injection conditions. The amount of unburned fuel is given by the second expression in (5.5). Note that $v_R > \sigma Y_{inj}/\gamma_f$, which follows from the inequality $n_f^{unb} > 0$ with n_f^{unb} from (5.5). Since $v_R < 1$, the necessary condition for complete oxygen consumption, counterpart to (3.50), becomes

$$Y_{inj}\sigma/\gamma_f < 1. \tag{5.11}$$

As it was mentioned in subsection 3.2.4, the equality $Y_{inj}\sigma/\gamma_f = 1$ corresponds to the resonant combustion. In both cases of complete oxygen and complete fuel consumption, $v_R \to 1$ as $Y_{inj}\sigma/\gamma_f \to 1$, i.e., the width of the hot zone shrinks to zero. Thus, by changing problem parameters, one combustion regime can change into the other passing through the resonance.

Note that the second condition in (5.3) coincides with condition (a) in (3.21). Case (b) corresponding to large diffusion is inappropriate in the case of complete oxygen consumption: the oxygen is completely expelled from the reaction zone by diffusion, leading to extinction.

5.2. Vaporization wave. The vaporization wave is a traveling wave with speed $v_V < 1$ consisting of an HL and a VP. In the leading VL, the liquid vaporizes at temperature $\theta \approx \theta_{vap}$. Then the HL follows, where the temperature raises from θ_{vap} to θ_h. Along the wave, $Y = 0$ and $n_f = 1$.

The HL and VL are analyzed in the same way as in sections 3.2.2 and 3.2.3, with v_R substituted by v_V. The temperature profile in the HL is found as

$$\theta = \alpha_0 + \alpha_1 \exp(-A\xi), \qquad A = v_V - 1 < 0. \tag{5.12}$$

Let us set $\xi = 0$ between the HL and VL. Since $\theta = \theta_h$ as $\xi \to -\infty$ and $\theta \approx \theta_{vap}$ at $\xi = 0$, we find $\alpha_0 = \theta_h$ and $\alpha_1 = \theta_{vap} - \theta_h$. Then the analysis of the VL yields the expressions

$$(\rho u)_{vap} = \frac{\sigma + \gamma_l v_V n_l^{vap}}{\sigma}, \quad X_{vap} = \frac{\gamma_l v_V n_l^{vap}}{\sigma + \gamma_l v_V n_l^{vap}}, \quad \theta_{vap} = \theta_h - \frac{v_V \beta n_l^{vap}}{1 - v_V}, \tag{5.13}$$

which are similar to (3.46), (3.47).

5.3. Condensation wave. The condensation wave has speed v_C. In this wave, $Y = 0$ and $n_f = 1$. The analysis of this wave is the same as in the complete fuel consumption case in section 3.3, yielding expressions (3.56), (3.58), and (3.59), with v_V instead of v_R. The latter two are

$$n_l^{vap} = \frac{\gamma_l v_C - \sigma X_{res}/(1 - X_{res})}{\gamma_l (v_C - v_V)}, \tag{5.14}$$

$$\theta_{vap}\,(v_C - 1 - \gamma_l v_V n_l^{vap}/\sigma) = \beta v_C (n_l^{vap} - 1). \tag{5.15}$$

5.4. Defining system of equations for the wave sequence. The two equations (5.7) and (5.10) determine the temperature θ_h and the combustion wave speed v_R for given injection conditions, through a single transcendental equation for v_R, which has to be solved numerically in the interval $0 < v_R < \sigma Y_{inj}/\gamma_f$. The unburned fuel concentration n_f^{unb} is given by (5.5).

Then the speeds of the vaporization and combustion waves v_V and v_C are determined by solving the system of two nonlinear equations (3.49), (5.15), where X_{vap}, θ_{vap}, and n_l^{vap} are substituted from (5.13), (5.14). This system must be solved numerically.

In addition to condition (5.11) for the combustion wave, the condition $n_l^{vap} \geq 1$ is required for the existence of the condensation wave.

5.5. Numerical results for typical reservoir data. The necessary condition for complete oxygen consumption regime (5.11) in dimensional form becomes $Y_{inj} < n_f^{res} c_g / C_m$. It is satisfied for either large fuel or low air concentrations. We will

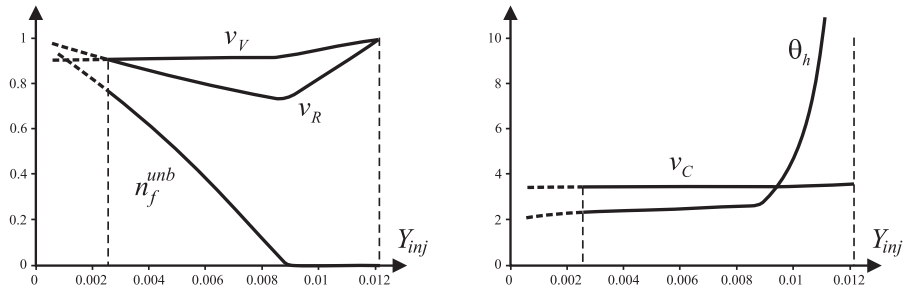

FIG. 7. *Nondimensional solution parameters depending on the initial oxygen fraction* Y_{inj}.

consider the data from Table 1, except that Y_{inj} is varied. Then, condition (5.11) becomes $Y_{inj} < 0.0122$. This means that the injected gas must contain a very small fraction of oxygen. Practically, one might think of injection of a mixture of air with flue gases. Solving the equations as described in the previous subsection for $0 < Y_{inj} < 0.0122$, we obtain the solution parameters, i.e., the wave speeds v_R, v_V, v_C, and intermediate states θ_h, n_f^{unb}, θ_{vap}, n_l^{vap}, X_{vap}; see Figure 7.

The interval $0.009 < Y_{inj} < 0.0122$ corresponds to the resonant regime when the combustion temperature grows and becomes very large for $Y_{inj} \approx 0.0122$. In this region $n_f^{unb} \approx 0$, so not only all oxygen is consumed, but almost all fuel is consumed as well. In the interval $0.0025 < Y_{inj} < 0.009$, the combustion temperature and wave speed remain almost constant: $\theta_h \approx 2.5$ (500 C°) and $v_R \approx 1$. This looks surprising, since the oxygen fraction Y_{inj} varies substantially. Such a behavior is explained by the change of speed difference $v_V - v_R$. This is so because most of the heat generated in the combustion goes into the hot zone, whose width grows in time proportionally to $v_V - v_R$. At $Y_{inj} = 0.0025$, the combustion and vaporization wave speeds coincide, so for $Y_{inj} < 0.0025$ the solution does not have the form we studied (the condition $v_R < v_V$ is violated). This means that the combustion is quenched by the liquid for $Y_{inj} < 0.0025$ if the liquid is not combustible. If the liquid is combustible, another combustion regime may appear. Note that, when approaching the singular point $Y_{inj} \approx 0.0025$, speeds v_R and v_V get closer, allowing the waves to interact for a long time. Thus, the time required for development of the steady combustion regime from a certain initial data increases. This means that the ignition becomes problematic.

The parameters in the vapor zone θ_{vap}, n_l^{vap}, X_{vap} (not shown in Figure 7) exceed very slightly their initial values in the reservoir, so the effect of vaporization/condensation in the vapor zone is small. The condensation wave speed also does not change much; $v_C \approx 3.5$. Finally, we mention that the numerical simulation of the original PDE system performed for $Y_{inj} = 0.007$ confirmed the analytical results with high accuracy.

6. Conclusion. Filtration combustion was considered in the case when air is injected behind the combustion wave into a porous medium containing a solid fuel and some amount of liquid, e.g., water or light oil. Understanding the behavior of this liquid in the vaporization/condensation process ahead of the combustion wave is of practical importance, for example, in designing prospective methods of oil recovery. On the other hand, the liquid may influence the combustion wave, changing its speed or leading to extinction.

In this paper, we studied two different solutions in the form of wave sequences that are typical for combustion in wet reservoirs. All the waves in these solutions are

described analytically, reducing the problem to solving a system of nonlinear transcendental equations. For typical reservoir data, we performed numerical simulation that confirmed the analytical results and studied the solution parameters depending on the fuel and injected oxygen concentrations. According to the computations, the presence of the liquid has a small influence on the combustion temperature. This is a natural conclusion when the heat needed for vaporization is much smaller than the heat released in the combustion. On the contrary, the wave speeds are sensitive to the liquid concentration. It is shown that the concentration of liquid increases in the vapor zone that lies between the combustion and condensation waves. However, this increase is not large and does not lead to any dramatic phenomena like extinction (at least for the data considered).

An interesting regime is detected when the injected air contains a very small amount of oxidizer (oxygen). In this regime, not all solid fuel is consumed in the reaction. Surprisingly, the combustion speed and temperature appear to be almost independent of the (small) oxygen concentration. However, further decrease of injected oxygen concentration leads to extinction. Note that the combustion temperature remains high for solutions in the neighborhood of the extinction point, and the extinction originates from the interaction of the combustion and vaporization waves.

In this paper we assumed that the liquid in the reservoir is immobile, which is true if only small amounts of liquid are present initially. Since the combustion wave speed is usually very low, one can expect that mobile liquid will be displaced by the injected air, without interacting with the combustion wave. This case, however, requires study.

REFERENCES

[1] I. Y. Akkutlu and Y. C. Yortsos, *The dynamics of in-situ combustion fronts in porous media*, Combust. Flame, 134 (2003), pp. 229–247.

[2] A. P. Aldushin, I. E. Rumanov, and B. J. Matkowsky, *Maximal energy accumulation in a superadiabatic filtration combustion wave*, Combust. Flame, 118 (1999), pp. 76–90.

[3] A. Bayliss and B. J. Matkowsky, *From traveling waves to chaos in combustion*, SIAM J. Appl. Math., 54 (1994), pp. 147–174.

[4] R. B. Bird, W. E. Stewart, and E. N. Lightfoot, *Transport Phenomena*, 2nd ed., Wiley, New York, 2002.

[5] J. Bruining and M. Marchesin, *Nitrogen and steam injection in a porous medium with water*, Transp. Porous Media, 62 (2006), pp. 251–281.

[6] D. N. Dietz and J. Weijdema, *Wet and partially quenched combustion*, in Proceedings of the 42nd Annual SPE of AIME Fall Meeting, Houston, 1967, Paper SPE-1899.

[7] E. L. Isaacson, D. Marchesin, and B. J. Plohr, *Transitional waves for conservation laws*, SIAM J. Math. Anal., 21 (1990), pp. 837–866.

[8] D. Marchesin and A. A. Mailybaev, *Dual-family viscous shock waves in n conservation laws with application to multi-phase flow in porous media*, Arch. Ration. Mech. Anal., 182 (2006), pp. 1–24.

[9] B. J. Matkowsky and G. Sivashinsky, *Propagation of a pulsating reaction front in solid fuel combustion*, SIAM J. Appl. Math., 35 (1978), pp. 465–478.

[10] D. A. Schult, B. J. Matkowsky, V. A. Volpert, and A. C. Fernandez-Pello, *Forced forward smolder combustion*, Combust. Flame, 104 (1996), pp. 1–26.

[11] D. A. Schult, A. Bayliss, and B. J. Matkowsky, *Traveling waves in natural counterflow filtration combustion and their stability*, SIAM J. Appl. Math., 58 (1998), pp. 806–852.

[12] I. W. Smith, *The intrinsic reactivity of carbons to oxygen*, Fuel, 57 (1978), pp. 409–414.

[13] C. W. Wahle, B. J. Matkowsky, and A. P. Aldushin, *Effects of gas-solid nonequilibrium in filtration combustion*, Combust. Sci. Tech., 175 (2003), pp. 1389–1499.